ARTICLE NO. 80-4109

Decay of Transverse Acoustic Waves in a Pulsed Gas Laser

Vijay A. Kulkarny*
TRW DSSG, Redondo Beach, Calif.

The long-term behavior of transverse acoustic waves in the cavity of a pulsed gaseous laser is investigated. The waves generated subsequent to a pulse by the protective inert gas streams along the walls and windows are analyzed in a straight duct configuration with nonlinear wave techniques used in sonic boom poblems. A decaying sawtooth waveform containing a shock wave is found to reverberate in the cavity transverse to the flow direction. For the asymptotic decay at large time t, (p/p_∞), the relative pressure perturbation in the transverse wave varies as the 2/5 power of $\{(p_0/p_\infty) \times [\ell\Delta/(ct)^2]\}$. Here (p_0/p_∞) is the relative overpressure resulting from the pulse, and c is the speed of sound in the gas. The length of the cavity along the flow axis is ℓ and the thickness of each inert layer is $\Delta/2$. However, this decay is rather slow and, in most lasers, additional attenuation must be provided by the acoustic suppressors primarily meant for waves in the flow direction.

Introduction

IN some repetitively pulsed gas phase lasers, the active laser gas is kept away from the windows and walls with coflowing streams of cold and inert gas called curtains. In other lasers, such cold layers occur near the lateral boundaries due to nonuniform energy deposition or reaction initiation. The lateral interface between the active gas and the cold gas gives rise to transverse pressure waves in the cavity as the active gas, when pulsed, instantaneously heats up at constant volume and consequently builds up pressure. The resulting violent interactions between the inhomogeneous fluid and the finite amplitude pressure waves and shock waves are highly nonlinear multidimensional phenomena which are extremely complex to deal with in full detail. However, the problem becomes tractable under approximations, when the ensuing transverse reverberation subsides in time, as the energy is channeled away by the waves which mainly travel along the duct. Understanding the decay of the transverse waves is very important since the density perturbations due to the waves in the cavity degrade the coherence of the laser beam for succeeding pulses. The acoustic behavior of the residual transverse waves can be predicted using approximate analysis. As is well known in acoustics, the linear formulation performs well at predicting the long-term or far-field behavior of diverging waves, even though they may be strongly nonlinear at the source. Major nonlinear effects can then be accounted for by correcting the characteristics. Similar approaches have worked well in far-field explosion waves and sonic boom problems.[1] Here this approach is demonstrated in a simplified situation. First, linear estimates of the long-term behavior of the transverse oscillations are obtained, which are then corrected for the dominant nonlinear effects.

The Problem

The geometry of the initial value problem of the pressure wavefield is shown in Fig. 1. In order to obtain analytical solutions we make the following simplifications:

1) Assume a straight one-dimensional duct, i.e., neglect the rest of the flow system. Consider straight-duct flow with no curtains parallel to the plane of the figure. Under these circumstances, the wavefield simply convects with the mean flow, and is solved for in that moving frame of reference.

Received July 17, 1979; revision received March 24, 1980.

Index categories: Lasers; Shock Waves and Detonations.
*Member of Technical Staff, Energy Technology Department.

2) Assume linearity of pressure variations, which is not valid for short times, but will be so in long time when the wave amplitudes decay, but perhaps with a slightly misplaced origin (temporal and spatial) for the waves.

3) Assume the gas is uniform throughout, i.e., no changes occur in acoustic properties (sound speed and impedance) in the entire duct.

It is important at this point to emphasize the differences from real pulse lasers. Pulse lasers employ a variety of sophisticated acoustic attenuation devices to suppress the waves traveling along the duct, and other flow devices for proper control of the gas flow. These are bound to have a significant influence on the transverse waves. Also, in the real system, the acoustic properties of the cavity gas (which has lased) differ from the rest of the gas. It is very difficult to account fully for such complex effects with any degree of generality. The simple analysis presented here characterizes the transverse waves in the absence of any dissipative devices and inhomogeneities. This may influence the choice of attenuation techniques to handle the problem of transverse waves.

Linear Wavefield

The development of the various wavefronts and diffraction regions in the two-dimensional acoustic wavefield, according to the linear theory[2] assuming a constant wavespeed, can be described very easily as shown in Figs. 2-5. Here the various wavefronts and boundaries are marked as follows:

A—expansion wave from the lateral interface E, $\delta p = -p_0/2$

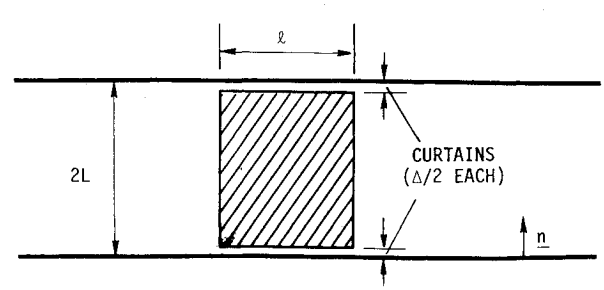

Fig. 1 Geometry of initial value problem.

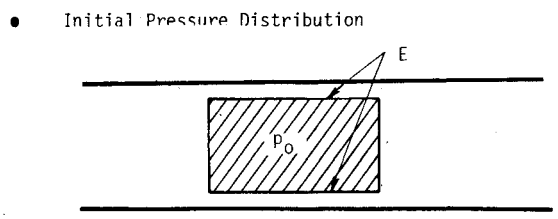

Fig. 2 Initiation of waves from pressure distribution.

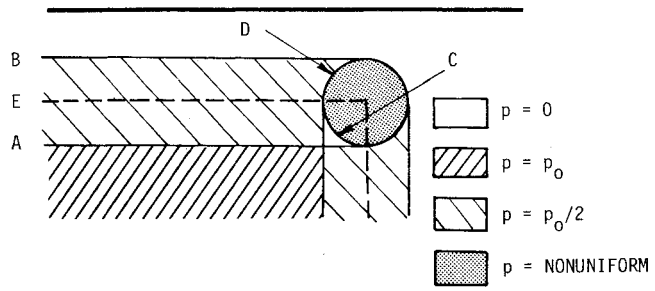

Fig. 3 Details of diffraction near the corners.

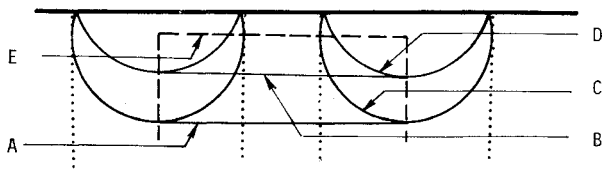

Fig. 4 Reflection from side walls.

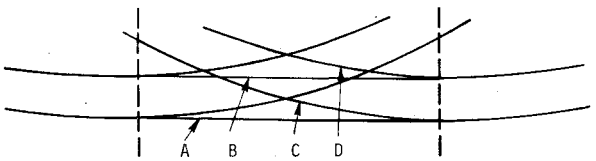

Fig. 5 Transverse wave after many reflections.

B—compression wave from the lateral interface *E*, $\delta p = +p_0/2$

C,D—front of the nonuniform pressure zero due to diffraction from the corner, where $p \rightarrow p_0/4$ toward the center

E—boundary of initially pressurized region, lateral interface

In Fig. 3 the pressure field is indicated by shading. The diffraction front is highly nonuniform and changes pressure in a parabolic fashion. Further, portion C is compressive, whereas portion D is expansive.

Figure 4 shows the waves after the first reflection from the duct wall. Only half the wavefield is shown for simplicity, since the other half is symmetric. The wavefronts of the axial motion are shown dotted as they are of minor importance to the transverse waves.

The basic geometry of the transverse wave does not change much in time despite many reflections, except the radii of the diffraction fronts C and D become larger continuously, and they become indistinguishable from fronts A and B,

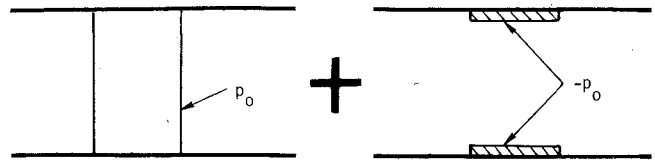

Fig. 6 Separation of one-dimensional initial value problem.

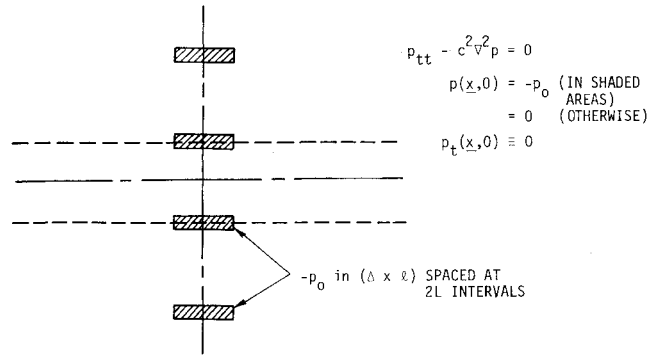

Fig. 7 Transformed problem in infinite medium.

respectively. In Fig. 5 the wave is shown without reference to the walls and the lateral interfaces. The vertical dashed lines correspond to the axial extent of the region of initial overpressure. The notation for the various wavefronts is the same as above.

Transformation of the Linear Problem

Under the assumptions made above, the pressure field $p(x,t)$ obeys

$$p_{tt} - c^2 \nabla^2 p = 0 \tag{1}$$

with $\hat{n} \cdot \nabla p = 0$ on the walls.

The distribution of initial values, shown in Fig. 1, may be separated into two parts as shown in Fig. 6, since the problem is linear and therefore allows superposition.

Clearly the first part generates a one-dimensional wavefield along the duct which can be adequately understood with well-known techniques[3-7] and therefore is of no concern here. The second part generates the two-dimensional decaying waves of interest, which reverberate transversely in the cavity. The second problem can be further transformed by removing the boundaries from considerations of symmetry. We then have an infinite sequence of low-pressure areas in an infinite medium as shown in Fig. 7. Note $\hat{n} \cdot \nabla p \equiv 0$ on the dashed lines representing the walls, by symmetry. Also, by symmetry, the center is a node of the acoustic velocity fluctuations and the pressure fluctuation is maximum there. This is because the upward-going and downward-going waves arrive at the center in phase due to symmetry. Problems of this nature can be solved using an existing general solution of the wave equation in terms of initial values. This solution is described below.

Poisson's Integral of the Wave Equation

Consider the three-dimensional pressure field[2]

$$p_{tt} - c^2 \nabla^2 p = 0$$

$$p(\vec{x},0) = P(\vec{x}), \quad p_t(\vec{x},0) = P_t(\vec{x}) \tag{2}$$

Then the solution is given by:

$$p(\vec{x},t) = \frac{\partial}{\partial t}\{tM_{\vec{x},t}[P(\xi)]\} + tM_{\vec{x},t}[P_t(\xi)] \tag{3}$$

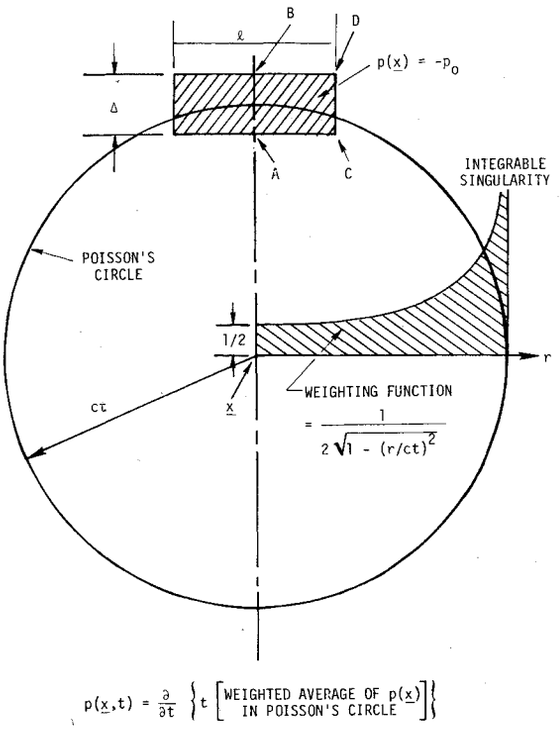

Fig. 8 Interpretation of Poisson integral.

where

$$M_{\bar{x},t}[\phi(\bar{\xi})] = \frac{1}{4\pi(ct)^2}\int_{S_{ct}(\bar{x},t)} \phi(\bar{\xi})\,dS$$

and $S_{ct}(\bar{x},t)$ is a sphere of radius ct with center $\bar{x}$ and $M_{\bar{x},t}[\phi(\bar{\xi})]$ is the average of ϕ on the surface of the sphere. In two-dimensional problems, $M_{\bar{x},t}$ reduces as:

$$M_{\bar{x},t}[\phi(\bar{\xi})] = \frac{1}{\pi(ct)^2}\int_{\sigma_{ct}(\bar{x},t)} \frac{\phi(\bar{\xi})\,d\sigma}{2\sqrt{1-(|\bar{x}-\bar{\xi}|/ct)^2}} \qquad (4)$$

where $\sigma_{ct}(\bar{x},t)$ is a circle of radius ct with center $\bar{x}$ and $M_{\bar{x},t}[\phi(\bar{\xi})]$ is the weighted average within the circle.

The application of the Poisson integral to find the wave from a single area of underpressure is illustrated in Fig. 8. The Poisson circle is shown located on the axis of symmetry for the purpose of calculations done in the next section. As the Poisson circle expands with time, it passes over the points A, C, B, and D, which generate the corresponding wavefronts described previously. As mentioned here, the weighting function for the average is singular at the circle. However, the singularity is integrable, and no special handing techniques are necessary if the evaluation is carried out in suitable variables. It is easy to see that the weighting function results from the projection of the contributions of the two area elements on the two sides of the Poisson's sphere in three dimensions. Physically, Poisson's solution can be interpreted as summing the pressure waves produced by little sources on the surface of the sphere. The initial pressure distribution is equivalent to a distribution of instantaneous sources activated at the initial instant. Then, at time t, only the waves from the sources on the sphere occur simultaneously at the center of the sphere.

Application of Poisson's Solution

The central region of the transformed problem corresponds to the laser cavity. The waves which occur here after a long time originate from low-pressure regions lying far away. This implies that the transverse waves have reflected back and forth between the walls many times. The Poisson integral can be approximated in this case to find the acoustic radiation at large distances from a small region of initial underpressure. Clearly in this limit, the wave diverges radially in two dimensions, and decays in accordance with geometrical optics; i.e., its amplitude varies as $r^{-1/2}$, where r is its distance from the source. This can be shown from the Poisson integral as follows:

$$p(\bar{x},t) = \frac{\partial}{\partial t}[tM_{\bar{x},t}(-p_0)]; \quad P_t(\bar{x},0) \equiv 0$$

Suppose the minimum distance from the point of interest to the region of underpressure is r_0; the region extends a distance Δ along the direction of r_0 and a distance $\ell \cdot f(r)$ transverse to it. The solution will show a perturbation only after time $t > r_0/c$. Thus a long-time or large distance approximation implies:

$$\Delta, \ell \ll r_0, ct$$

Then,

$$p(r_0,t) \simeq \frac{\partial}{\partial t}\left[\frac{-p_0\ell}{\pi c}\int_{r_0}^{ct} \frac{f(r)\,dr}{2\sqrt{(ct)^2-r^2}}\right] \qquad (5)$$

If $\eta = (ct-r)/\Delta$ and $\eta_0 = (ct-r_0)/\Delta$, where $\eta_0 < 1$

$$p(r_0,t) \simeq \frac{-p_0\ell}{2\sqrt{2}\pi}\sqrt{\frac{\Delta}{r_0}}\frac{\partial}{\partial(ct)}\int_0^{\eta_0} \frac{f(\eta)\,d\eta}{\sqrt{\eta}\sqrt{1+\eta(\Delta/2r_0)}}$$

$$\simeq \frac{-p_0}{2\sqrt{2}\pi}\frac{\ell}{\sqrt{r_0\Delta}}\frac{f(\eta)}{\sqrt{\eta}} \qquad (6)$$

Here $f(\eta)$ depends upon the details of the geometry of the region of initial underpressure and the Poisson circle, and eliminates the singularity at the leading edge of the wave, as can be shown from rigorous analysis. To find the scale of the perturbation it is sufficient to assume that the factor $f(\eta)/\sqrt{\eta}$ is of order unity. Thus, using $r_0 \simeq ct$, the magnitude of the pressure fluctuation in the central region can be estimated as

$$p(t) \simeq \frac{p_0}{2\sqrt{2}\pi}\left[\frac{(\ell/\Delta)}{(ct/\ell)}\right]^{1/2} \qquad (7)$$

It should be noted that, in this approximation, it is implicitly assumed that $\ell/\Delta < \sqrt{ct/\Delta}$. The analysis must be done differently, if ℓ is large and t is small enough to violate this condition. However, for any ℓ/Δ, the above behavior of the pressure fluctuations becomes valid as $ct \simeq r_0 \to \infty$.

The form of the pressure pulse resulting from one of the lateral interfaces, observed after a long time at a point axially in the middle of the cavity is shown in Fig. 9. Here T is the time measured since the arrival of A, the first wavefront. Thus $T = t - (r_0/c)$. Clearly, the diffractions from the left and the right arrive simultaneously at this point. Thus there are only four distinct wavefronts observed at the point, in the sequence A, C, B, D. Front A results from the plane pressure discontinuity at the lateral interface. It is plane and carries a discontinuous presesure change $\delta p = -p_0/2$. Front C heads the nonuniform regions of diffraction. The pressure variation during this phase is obtained from the Poisson integral.

For $(ct-r_0) < \Delta$ and $r_0 \simeq ct$, as shown before in Eq. (6),

$$p(r_0,t) \simeq \frac{-p_0}{2\sqrt{2}\pi}\frac{\ell}{\sqrt{r_0\Delta}}\frac{f(\eta)}{\sqrt{\eta}} \qquad (8)$$

The pressure variation shown in the figure can be verified by replacing $f(\eta) = 1$ and $r_0 \simeq ct$. Here $T = t - (r_0/c) = \Delta\eta/c$. The front B is the reflection of the counterpart of A, which is

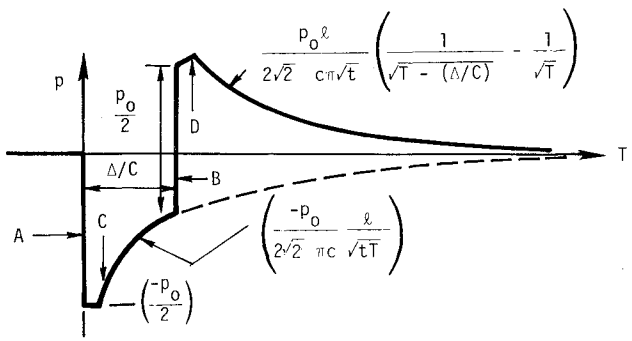

Fig. 9 Linear waveform.

plane and carries a discontinuous pressure change $p=+p_0/2$. This merely becomes superposed on the pressure variation due to front C, until front D arrives. The combined pressure variation due to fronts C and D can be determined from the Poisson integral, but it is simpler to find by the following argument:

The area of initial underpressure $-p_0$ and of size $\ell \times \Delta$ may be considered as superposition of two different initial value regions for the linear problem. The first has underpressure $-p_0$ and width ℓ, begins at distance r_0 from the point of interest, and extends to infinity. The second region has overpressure p_0 and width ℓ, begins at distance $(r_0+\Delta)$ from the point of interest, and extends to infinity. The wave from the first region results in fronts A and C, with continuation of the $T^{-1/2}$ behavior shown by a dashed line in Fig. 9. The wave from the second region contains the fronts B and D, and is identical to the other wave except it is inverted and lags behind by distance Δ and time (Δ/c). The superposition of the two waves produces the signals generated by the finite area of underpressure.

Although this waveform slowly changes as it travels, the behavior of its integral, the total impulse in the wave, remains unaltered. This is true even when the wave is nonlinear and decays rapidly by formation of finite amplitude shocks. This is explained and used later when correcting for the nonlinear effects. The impulse is found as follows:

$$I=\int p(r_0,t)\,dt = tM_{r_0,t}(-P_0) \tag{9}$$

When $ct \gg r_0 \gg \Delta$, it is easily shown that,

$$I \sim \frac{-P_0 \ell \Delta}{2\pi c^2 t}\int_0^1 f(\eta')\,d\eta' \to 0 \text{ as } t\to\infty t \tag{10}$$

Thus the total impulse in wave is vanishingly small for large times. Physically, the waveform consists of a superposition of two equal and opposite decaying pressure signatures with a phase lag Δ/c. Clearly, the integral of such a waveform will vanish as $(ct/\Delta) \ll 1$.

Nonlinear Distortion of the Waveform

It is well known in acoustics that the first deviations from linearity occur in misplacement of various characteristics. The characteristics carry a signal at the local speed of sound relative to the local fluid, which may be in motion also. Since the signal itself changes the local sound speed and fluid velocity by isentropic compression or rarefaction, different characteristics carrying different levels of the signal travel at different speeds. When compared to a linear solution, therefore, the characteristics occur at different locations, and their misplacement grows continuously with elapsed time or traveled distance. Thus for finite amplitude waves, the predominant manifestation of nonlinearity, i.e., the amplitude dependence of wavespeed, shows up as a distortion of the waveform in the far field. Since the wavespeed increases

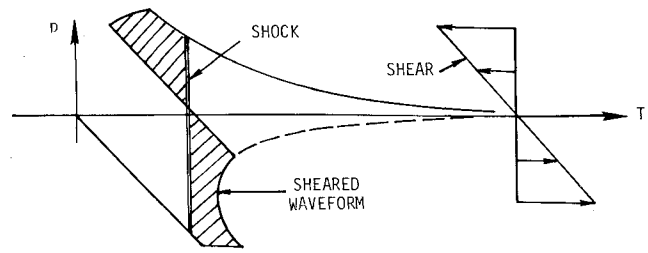

Fig. 10 Nonlinear distortion of waveform.

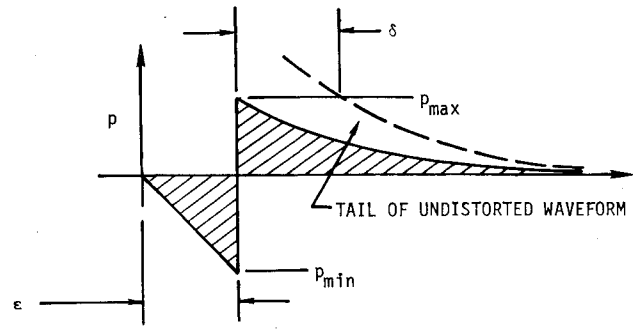

Fig. 11 Distorted waveform.

with compression and decreases with rarefaction, the distortion simply amounts to a continuous shearing of the linear waveform, as shown in Fig. 10.

As the amount of shear grows with time, all solutions tend to become multivalued. However, pressure waves cannot produce multivalued solutions for physically obvious reasons. For the solution to become multivalued, it is necessary that the gradient in pressure tend to infinity at some point. When this happens, in the narrow region of the large pressure gradient, dissipative processes become significant and prevent further shearing of the pressure profile in this zone. This zone, which appears as a discontinuity in pressure due to its extreme narrowness, is a shock wave. Unless very strong in amplitude, the shock wave travels at the mean velocity of the characteristics immediately ahead of it and behind it, so that it catches up with the waves ahead of it, whereas the waves behind it keep merging in. As these processes modify the shock amplitude, more and more of the original wavefield disappears (hatched region) into the shockwave, leaving a simple asymptotic sawtooth-like waveform shown in Fig. 10.

For the weakly nonlinear waves under consideration, the wavespeed varies linearly with pressure. The mean speed of the shock wave then implies conservation of the impulse (time integral of the pressure variations) in the wave. Therefore, the location and the amplitude of the shock wave can be determined by matching the areas of the disappeared parts of the distorted pressure signature. (Obviously, the process of distortion by shearing also preserves the impulse in the wave.) These areas are shown hatched in Fig. 10.

Nonlinear Correction and Wave Decay

For isentropic pressure waves in a gas, the characteristic wave speed is $(c'+u)$, where c' is the local sound speed relative to the gas and u is the local gas velocity. Using Riemannian theory for plane waves, we obtain:

$$c' = c + \frac{\gamma-1}{2}u \tag{11}$$

Thus

$$c'+u = c+\frac{\gamma+1}{2}u = c+\frac{\gamma+1}{\gamma-1}(c'-c)$$

From the isentropic relationship between variables of state

$$\frac{c'}{c}=\left(1+\frac{p}{p_\infty}\right)^{\frac{\gamma-1}{2\gamma}}$$

where p_∞ is the pressure in the undisturbed medium. Eliminating c' in terms of p, the amplitude,

$$c'+u=c\left\{1+\frac{\gamma+1}{\gamma-1}\left[\left(\frac{p}{p_\infty}+1\right)^{\frac{\gamma-1}{2\gamma}}-1\right]\right\} \tag{12}$$

For the weak waves of interest in this problem, this can be expanded and simplified to

$$c'+u=c\left[1+\frac{\gamma+1}{2\gamma}\left(\frac{p}{p_\infty}\right)-\frac{(\gamma+1)^2}{4\gamma(\gamma-1)}\left(\frac{p}{p_\infty}\right)^2+0\left(\frac{p}{p_\infty}\right)^3\right] \tag{13}$$

To find the long-term behavior of the waves we retain only the linear term in the expansion. Thus, a characteristic carrying amplitude p travels as

$$\frac{dr}{dt}=c\left[1+\frac{\gamma+1}{2\gamma}\left(\frac{p}{p_\infty}\right)\right] \tag{14}$$

Integration of this equation to find the correct location of the characteristic, however, is complicated by the fact that the amplitude on a given characteristic T decays as $(ct)^{-1/2}$ due to radial spreading. We apply the distortion only to the compressive tail of the linear waveform, for which

$$\frac{p}{p_\infty}=\frac{1}{2\sqrt{2}\pi}\cdot\frac{p_0}{p_\infty}\cdot\frac{\ell}{\sqrt{ct}}\cdot\left(\frac{1}{\sqrt{cT-\Delta}}-\frac{1}{\sqrt{cT}}\right)=\frac{p'(cT)}{\sqrt{ct}} \tag{15}$$

Here the fixed value of T represents a given characteristic, which then travels as

$$\frac{dr}{d(ct)}=1+\frac{\gamma+1}{2\gamma}\cdot\frac{p'(cT)}{\sqrt{ct}} \tag{16}$$

Therefore

$$r=ct+\frac{\gamma+1}{2\gamma}\times p'(cT)\times 2\sqrt{ct} \tag{17}$$

Then, at an instant t, the correction for the nonlinear distortion is displacement within the waveform of a characteristic from cT to cT', where

$$cT'=cT+\frac{\gamma+1}{2\gamma}\times p'(cT)\times 2\sqrt{ct} \tag{18}$$

In order to fit a shock into the distorted waveform between the leading rarefaction and the compressive tail, the total impulse in the wave must be preserved. The total impulse is vanishingly small as shown by Eq. (10). This implies that the shock can be fit in by matching the shaded areas in the rarefactional and the compressive portions of the waveform as shown in Fig. 11.

The area under this distorted waveform can be easily obtained by shearing the waveform backwards to the undistorted shape. This process preserves the area and simplifies the integration. In Fig. 12, the total impulse, which must vanish, is the sum total of the three areas labeled F, G, and H. Altogether, four conditions are required to determine the four unknowns, p_{max}, p_{min}, ϵ, and δ. The distortion of the compressive tail is known, and implies two conditions:

$$c\delta=\frac{\gamma+1}{2\gamma}\times p'[c(\epsilon+\delta)]\times 2\sqrt{ct}=\frac{\gamma+1}{2\gamma}\times\frac{p_{max}}{p_\infty}\times 2ct \tag{19}$$

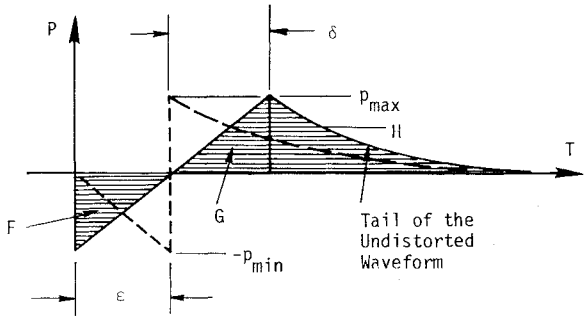

Fig. 12 Evaluation of impulse.

The tilted shock implies a geometrical condition:

$$p_{max}/p_{min}=\delta/\epsilon \tag{20}$$

The conservation of total impulse provides a final condition:

$$F+G+H=0 \tag{21}$$

Now

$$G=\frac{1}{2}\delta p_{max}=\frac{\gamma p_\infty}{\gamma+1}\frac{\delta^2}{2t} \tag{22}$$

$$F=-\frac{1}{2}\epsilon p_{min}=-(\epsilon/\delta)^2 \quad G=\frac{-\gamma p_\infty}{\gamma+1}\frac{\epsilon^2}{2t} \tag{23}$$

The area H under the compressive tail of the waveform is the following integral (since $\Delta \ll ct$):

$$H\simeq\frac{p_0}{\sqrt{2}\pi}\frac{\ell}{c}\frac{1}{\sqrt{ct}}\left[\sqrt{c(\epsilon+\delta)}-\sqrt{c(\epsilon+\delta)-\Delta}\right] \tag{24}$$

Thus Eq. (21) takes the form

$$\sqrt{2}\frac{\gamma+1}{\pi\gamma}\frac{p_0}{p_\infty}\frac{\ell\sqrt{ct}}{c^2}\left(\sqrt{c(\epsilon+\delta)}-\sqrt{c(\epsilon+\delta)-\Delta}\right)+(\delta^2-\epsilon^2)=0 \tag{25}$$

Using the known form of $p'(ct)$ for the compressive tail in the following condition for distortion given by Eq. (19),

$$\frac{p'[c(\epsilon+\delta)]}{\sqrt{ct}}=\frac{\gamma}{\gamma+1}\cdot\frac{\delta}{t} \tag{26}$$

we obtain:

$$\frac{\gamma+1}{2\sqrt{2}\pi\gamma}\frac{p_0}{p_\infty}\frac{\ell\sqrt{ct}}{c}\left(\frac{1}{\sqrt{c(\epsilon+\delta)-1}}-\frac{1}{\sqrt{c(\epsilon+\delta)}}\right)-\delta=0 \tag{27}$$

This condition, together with Eq. (25) on the impulse integral, represents two nonlinear equations to be solved simultaneously for ϵ and δ. We choose the following nondimensional forms

$$\frac{c(\delta+\epsilon)}{\Delta}=x;\quad\frac{c\delta}{\Delta}=y;\quad\frac{\gamma+1}{\sqrt{2}\pi\gamma}\frac{p_0}{p_\infty}\frac{\ell}{\Delta}\sqrt{\frac{ct}{\Delta}}=\beta \tag{28}$$

Then the equations become

$$2\beta(\sqrt{x}-\sqrt{x-1})+x(2y-x)=0 \tag{29}$$

$$\frac{1}{2}\beta\left(\frac{1}{\sqrt{x-1}}-\frac{1}{\sqrt{x}}\right)-y=0 \tag{30}$$

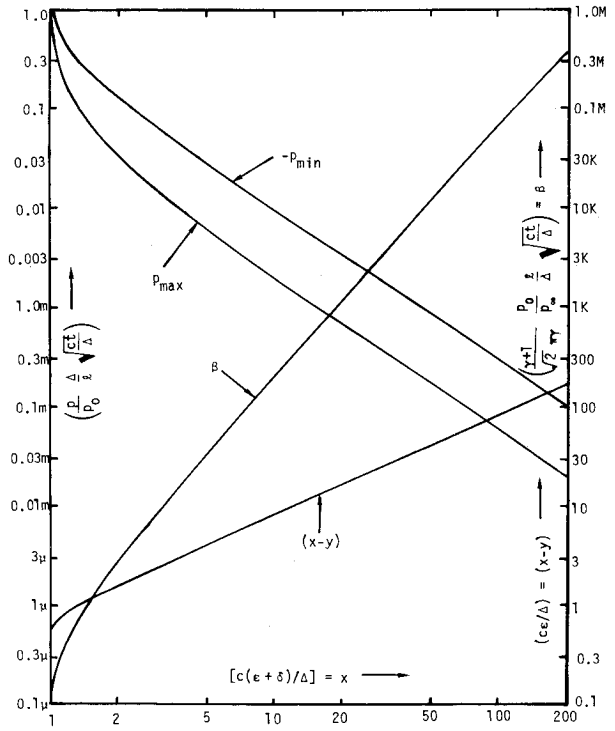

Fig. 13 Solution curves for dimensionless parameters.

These equations are easily solved for y and β as functions of x.

$$\beta = \frac{x^2\sqrt{x-1}}{\sqrt{x}\sqrt{x-1}+2-x} \sim \frac{2}{3}x^{\frac{5}{2}}\left[1+0\left(\frac{1}{x}\right)\right] \tag{31}$$

$$y = \frac{1}{2}\frac{x\sqrt{x}(\sqrt{x}-\sqrt{x-1})}{\sqrt{x}\sqrt{x-1}+2-x} \sim \frac{x}{6}\left[1+0\left(\frac{1}{x}\right)\right] \tag{32}$$

According to the distortion condition

$$y = \frac{c\delta}{\Delta} = \frac{\gamma+1}{\gamma}\frac{p_{\max}}{p_\infty}\frac{ct}{\Delta} = \sqrt{2}\pi\beta\frac{p_{\max}}{p_0}\sqrt{\frac{\Delta}{\ell}}\sqrt{\frac{ct}{\ell}} \tag{33}$$

$$\frac{p_{\max}}{p_0}\cdot\frac{\Delta}{\ell}\sqrt{\frac{ct}{\Delta}} = \frac{1}{2\sqrt{2}\pi}\left(\frac{1}{\sqrt{x-1}}-\frac{1}{\sqrt{x}}\right)$$

$$\sim \frac{x^{-3/2}}{4\sqrt{2}\pi}\left[1+0\left(\frac{1}{x}\right)\right] \tag{34}$$

$$\frac{p_{\min}}{p_0}\sqrt{\frac{\Delta}{\ell}}\sqrt{\frac{ct}{\ell}} = \frac{p_{\max}}{p_0}\sqrt{\frac{\Delta}{\ell}}\sqrt{\frac{ct}{\ell}}\left(\frac{x-y}{y}\right) = \frac{x-y}{\sqrt{2}\pi\beta} \tag{35}$$

The shock location within the wave is

$$(x-y) \sim \frac{5x}{6}\left[1+0\left(\frac{1}{x}\right)\right] \tag{36}$$

Also

$$\frac{p_{\min}}{p_0}\cdot\sqrt{\frac{\Delta}{\ell}}\sqrt{\frac{ct}{\ell}} \sim \frac{-5}{4\sqrt{2}\pi}x^{-3/2}\left[1+0\left(\frac{1}{x}\right)\right] \tag{37}$$

These solutions for the decay of the nonlinear transverse wave are shown graphically in the Fig. 13. The dimensionless parameters β, the shock location characteristic $(x-y)$, and the minimum and maximum pressures occurring just before and after the shock are displayed logarithmically as functions of x, the characteristic immediately behind the shock. The curves merge with their respective asymptotes for $x \gtrsim 20$. The validity of the analysis in the proximity of $x=1$ is doubtful, since the inherent assumptions become inaccurate or questionable in that region. However, the experience from the sonic boom problems indicates that the technique yields surprisingly good results even for rather short wave propagation times, and its accuracy continues to improve for longer times.

Conclusion

The two-dimensional transverse waves generated by the inactive wall layers in the cavity of a pulsed gas phase laser in a straight duct configuration decay in time due to spreading and nonlinear effects. An approximate linear analysis yields the waveform which reverberates in the cavity and decays as $t^{-1/2}$ because it diverges. The nonlinear effects modify this waveform and strongly enhance its decay.

In that case, the nonlinearity, the time, and the geometry couple into a single parameter β for which the waveform, the shock location, and the relative amplitudes (maxima and minima) can be determined. The asymptotic decay of the transverse wave scales with the different nondimensional parameters of the problem as given below:

Shock location in the wave:

$$\left(\frac{\epsilon}{t}\right) \sim \frac{5}{6}\left(\frac{3}{2}\frac{\gamma+1}{\sqrt{2}\pi\gamma}\right)^{2/5}\left[\left(\frac{p_0}{p_\infty}\right)\left(\frac{\ell}{ct}\right)^2\left(\frac{\Delta}{\ell}\right)\right]^{2/5} \tag{38}$$

Wave amplitudes:

$$\left(\frac{p_{\max}}{p_\infty}\right) \sim \frac{1}{4\sqrt{2}\pi}\left(\frac{3}{2}\frac{\gamma+1}{\sqrt{2}\pi\gamma}\right)^{-3/5}\left[\left(\frac{p_0}{p_\infty}\right)\left(\frac{\ell}{ct}\right)^2\left(\frac{\Delta}{\ell}\right)\right]^{2/5} \tag{39}$$

$$\left(\frac{p_{\min}}{p_\infty}\right) \sim -5\left(\frac{p_{\max}}{p_\infty}\right)$$

This inherent decay of the transverse waves is quite slow for most laser applications,† which therefore must employ highly effective acoustic attenuation devices. The analysis provides the nature and level of disturbance in the absence of attenuators and should be useful in determining the degree and the type of attenuation required to suppress the transverse waves.

Acknowledgment

The work reported here was performed under contract to the Department of Energy, Division of Laser Fusion, Contract DE-AC08-78DP40070.

References

[1] Whitham, G. B., *Linear and Nonlinear Waves*, John Wiley & Sons, New York, 1974, pp. 312-338.

[2] Friedlander, F. G., *Sound Pulses*, Cambridge University Press, Cambridge, 1958, pp. 1-67 and 108-146.

[3] Ausherman, D. R., Alber, I. E., and Baum, E., "Acoustic Suppression in a Pulsed Chemical Laser," AIAA Paper 78-237, Huntsville, Ala., Jan. 16-18, 1978.

[4] Thayer, W. J., III, Buonadonna, V. R., and Sherman, W. D., "Pressure Wave Suppression for a Pulsed Chemical Laser," AIAA Paper 78-1216, Seattle, Wash., July 10-12, 1978,

[5] Hogge, H. D. and Crow, S. C., "Flow and Acoustics in Pulsed Excimer Lasers," presented at AIAA Conference on Fluid Dynamics of High Power Lasers, Cambridge, Mass., Oct. 31-Nov. 2, 1978.

[6] Srivastava, B. N., Knight, C. J., and Zappa, O., "Acoustic Suppression in a Pulsed Laser System," AIAA Paper 79-0209, New Orleans, La., Jan. 15-17, 1979.

[7] Schwartz, J., Kulkarny, V. A. and Ausherman, D. R., "Pressure Wave Attenuation for Repetitively Pulsed Fusion Lasers," *Proceedings of the 12th International Symposium on Shock Tubes and Waves*, Jerusalem, Israel, July 1979.

†The isentropic density perturbations corresponding to the above pressure waveform must be integrated along the beam path to obtain the optical path difference function over the laser aperture. The wave is considered to be almost plane for this purpose, due to its large distance from the image source.